

## Identification of a Specific Inhibitor of nOGA – a Caspase-3 Cleaved *O*-GlcNAcase Variant during Apoptosis

Jing Li<sup>#</sup>, Zhonghua Li<sup>#</sup>, Tiehai Li, Lin Lin, Yan Zhang,  
Lina Guo, Yan Xu, Wei Zhao\*, and Peng Wang\*

College of Pharmacy, State Key Laboratory of Medicinal Chemical Biology and Tianjin Key Laboratory  
of Molecular Drug Research, Nankai University, Tianjin 300071, China; fax: +86-22-2350-7880;  
E-mail: wzhao@nankai.edu.cn; pwang@nankai.edu.cn

Received July 8, 2011

Revision received September 26, 2011

**Abstract**—*O*-Linked *N*-acetylglucosamine (*O*-GlcNAc) modification of serines/threonines on cytoplasmic proteins is a significant signal regulating cellular processes such as cell cycle, cell development, and cell apoptosis. *O*-GlcNAcase (OGA) is responsible for the removal of *O*-GlcNAc, and it thus plays a critical role in *O*-GlcNAc metabolism. Interestingly, OGA can be cleaved by caspase-3 into two fragments during apoptosis, producing an N-terminal fragment (1–413 a.a.), termed nOGA. Here, using 4-MU-GlcNAc (4-methylumbelliferyl 2-acetamido-2-deoxy- $\beta$ -D-glucopyranoside) as substrate, we found that the nOGA fragment retains high glycosidase activity. To probe the role of nOGA in apoptosis, it is essential to develop a potent and specific nOGA inhibitor. However, many reported inhibitors active at nanomolar concentrations (including PUGNAc, STZ, GlcNAc-statin, and NAG-thiazoline) against full-length OGA were not potent for nOGA. Next, we screened a small triazole-linked carbohydrate library and first identified compound **4** (4-pyridyl-1-(2'-deoxy-2'-acetamido- $\beta$ -D-glucopyranosyl)-1,2,3-triazole) as a potent and competitive inhibitor for nOGA. This compound shows 15-fold selectivity for nOGA ( $K_i = 48 \mu\text{M}$ ) over the full-length OGA ( $K_i = 725 \mu\text{M}$ ) and 10-fold selectivity over human lysosomal  $\beta$ -hexosaminidase A&B (Hex A&B) ( $K_i = 502 \mu\text{M}$ ). These results reveal that compound **4** can be used as a potent and selective inhibitor for probing the role of nOGA in biological systems.

DOI: 10.1134/S0006297912020113

**Key words:** *O*-GlcNAcase, isoforms, inhibitor, selectivity

*O*-GlcNAc, a single *N*-acetylglucosamine moiety, attached to serine or threonine residues of proteins via a  $\beta$ -*O*-glycosidic linkage, is an abundant, essential, and dynamic posttranslational modification in metazoans [1, 2]. Analogous to phosphorylation, *O*-GlcNAc to target proteins serves as a signaling regulation in cellular processes including cell cycle, nutrient sensing, and stress

response. Aberrant *O*-GlcNAcylation may be involved in the etiology of neurodegenerative disorders, diabetes mellitus, and cancer. The dynamic nature of *O*-GlcNAc and interplay with phosphorylation has enabled investigators to modulate intracellular *O*-GlcNAc levels to study its function [2, 3]. Although some genetic and pharmacological methods are available for manipulating *O*-GlcNAc levels, the most direct and useful strategy is by using small molecule inhibitors of *O*-GlcNAcase (OGA) [4].

OGA, belonging to GH84 family (<http://www.cazy.org>), is the only enzyme responsible for the cleavage of *O*-GlcNAc from proteins [2]. Human OGA exists in two isoforms: the full-length *O*-GlcNAcase (fOGA) and the spliced transcript variant of OGA (vOGA) [5]. fOGA, mainly located in cytoplasm, is a bifunctional enzyme consisting of two domains in which the N-terminus possesses *O*-GlcNAcase activity, while the C-terminus has histone acetyltransferase activity [6]. vOGA is the product of an alternatively spliced transcript of the *OGA* gene, which locates in the nucleus and lacks the C-terminal

**Abbreviations:** fOGA, full-length *O*-GlcNAcase; Hex A&B, human lysosomal  $\beta$ -hexosaminidase A&B; IPTG, isopropyl-L-thio- $\beta$ -D-galactopyranoside; LB, Luria–Bertani medium; LBNB, Luria–Bertani medium supplemented with NaCl and betaine; 4-MU-GlcNAc, 4-methylumbelliferyl 2-acetamido-2-deoxy- $\beta$ -D-glucopyranoside; nOGA, N-terminal fragment of *O*-GlcNAcase; OGA, *O*-GlcNAcase ( $\beta$ -exo-*N*-acetylhexosaminidase); *O*-GlcNAc, *O*-linked *N*-acetylglucosamine; PUGNAc, D-(2-acetyl-amido-2-deoxy-D-glucopyranosylidene)amino-*N*-phenylcarbamate; vOGA, variant of *O*-GlcNAcase.

<sup>#</sup> These authors contributed equally to this work.

\* To whom correspondence should be addressed.

histone acetyltransferase domain [5]. Interestingly, fOGA and vOGA can be cleaved by caspase-3 into two fragments during apoptosis, and an N-terminal fragment (a.a. 1-413, nOGA) preserves the *O*-GlcNAcase activity [7]. Although glycoside hydrolysis activity has been reported for the three forms previously, each form displays distinct catalytic efficiency [8, 9], indicating differential three-dimensional structure of the *O*-GlcNAcase domain. Therefore, efficient and selective small molecule inhibitors are urgently needed to study the features of different OGA isoforms.

To date, many OGA inhibitors have been developed and characterized including PUGNAc analogs, NAG-thiazolin analogs, and GlcNAc-statin analogs. Analyzing the inhibitory properties of these inhibitors, they are almost all active towards fOGA or vOGA and none are for nOGA [4]. Though nOGA is the N-terminal fragment of caspase-3 cleavage in apoptosis, it is still unclear whether this cleavage affects the glycosidase activity of fOGA and further apoptotic events of the cell. To properly interpret these questions, it is important to develop potent and specific small molecular inhibitors for nOGA.

The Cu(I)-catalyzed [3+2] azide-alkyne cycloaddition reaction to generate triazoles connecting azides and alkynes together with high yield under mild conditions is a highly versatile and effective strategy for the synthesis and identification of biologically active compounds having a number of biological activities [10, 11]. In addition, the triazole ring does not act merely as a “linker” fragment – it usually has favorable physicochemical properties that provide interaction with biological targets through hydrogen bonding and dipole–dipole and  $\pi$ -stacking interactions [12]. According to these features, a small triazole-linked carbohydrate library was screened in a search for efficient and selective inhibitors of nOGA.

## MATERIALS AND METHODS

**Bacterial strains, plasmids, and materials.** Human *O*-GlcNAcase cDNA (GenBank accession number AB014579) was kindly provided by Dr. Hart from the Medical School of Johns Hopkins University; *Escherichia coli* DH5 $\alpha$  was from Gibco-BRL Life Technology (USA); *E. coli* BL21(DE3) and pET-28a plasmid were from Novagen (USA); restriction enzymes were from Fermentas (USA); Ex Taq and Taq DNA polymerases and T4 ligase were from Takara (China); recombinant caspase-3 was from BIOMOL Research Laboratories (USA); human placenta  $\beta$ -*N*-acetylglucosaminidase A&B (A6152) and 4-MU-GlcNAc (4-methylumbelliferyl 2-acetamido-2-deoxy- $\beta$ -D-glucopyranoside) were from Sigma Aldrich (USA). Other chemicals were of the highest grade from commercially available sources.

**Plasmid constructions.** The *fOGA* and *nOGA* genes were amplified by polymerase chain reaction (PCR) using

the following primers and procedures. Since the N-terminal sequence was identical, one forward primer was used for amplification. The forward primer was 5'-CGCGCG-GCCGCGTGCAGAAGGAGAGTCAA-3' (*NotI*). The reverse primer for *fOGA* was 5'-GCGCTCGAGTTACAGGCTCCGACCAAGT-3' (*XhoI*) and for nOGA was 5'-GCGCTCGAGTTAATCAACTACACTT-3' (*XhoI*), respectively. The PCR fragments were then subcloned into pET28a vector with *NotI* and *XhoI* sites and produced recombinant plasmids: pET28a-*fOGA* and pET28a-*nOGA*. Subsequently, the recombinant plasmids were confirmed by restriction mapping and sequencing.

**Expression and purification of recombinant OGA isoforms.** *Escherichia coli* BL21(DE3) transformed with pET28a-*fOGA* or pET28a-*nOGA* was grown in Luria–Bertani (LB) and LBNB (LB medium supplemented with 0.5 M NaCl, 1 mM betaine) media supplemented with 50  $\mu$ g/ml kanamycin at 37°C overnight. The next day, the inoculated culture was added to 1 liter of LB medium and grown to OD<sub>600</sub> ~ 0.6 before induction with 0.025 and 0.1 mM IPTG (isopropyl-L-thio- $\beta$ -D-galactopyranoside). The bacteria were further grown for 10 h at 16°C at 150 rpm, harvested by centrifugation, and resuspended in 50 mM phosphate buffer, pH 8.0, 300 mM NaCl. Bacteria pellets were sonicated using a Vibra Cell Sonifier (Scientz-IID, China) with a 19-mm threaded probe. The sonication conditions were 10 sec per cycle (pulse on time 2 sec, pulse off time 8 sec), 40% output, and sonication for 30 min. Cell debris was removed by centrifugation (13,000g, 30 min, 4°C), and the supernatant was passed through a Ni<sup>2+</sup>-NTA (nickel-nitrilotriacetic acid) column (Qiagen, USA). After vigorous washing, the bound protein was eluted using 50 mM phosphate buffer, pH 8.0, 300 mM NaCl, and 300 mM imidazole. A Microcon YM-50/YM-100 micro-concentrator (Millipore, USA) device was used for buffer exchange and concentration. The recombinant protein was exchanged into 50 mM Tris-HCl buffer, pH 7.0, containing 1 mM dithiothreitol (DTT), 10% glycerol, and 150 mM NaCl. Protein concentration was estimated by the Bradford method [13]. The purity and apparent molecular mass were determined by SDS-PAGE [14].

**Generation of *O*-GlcNAcase antibody.** Using nOGA as antigen, we created a rabbit polyclonal antibody specific to the N-terminus of *O*-GlcNAcase from CWBIO company (China). The nOGA was expressed in *E. coli* and purified with Ni-NTA affinity chromatography and size exclusion chromatography, respectively. SDS-PAGE verified the molecular mass (55 kDa) and the purity (>95%), and the purified nOGA was used to immunize New Zealand rabbits. Subsequently, anti-serum was passed through antigen-coupled columns (CNBr-activated Sepharose 4B beads) three times, and antibody was eluted by 100 mM Tris, pH 8.0. Western blotting and ELISA assay identified the specificity and sensitivity of this antibody (the titer was 1 : 80,000).

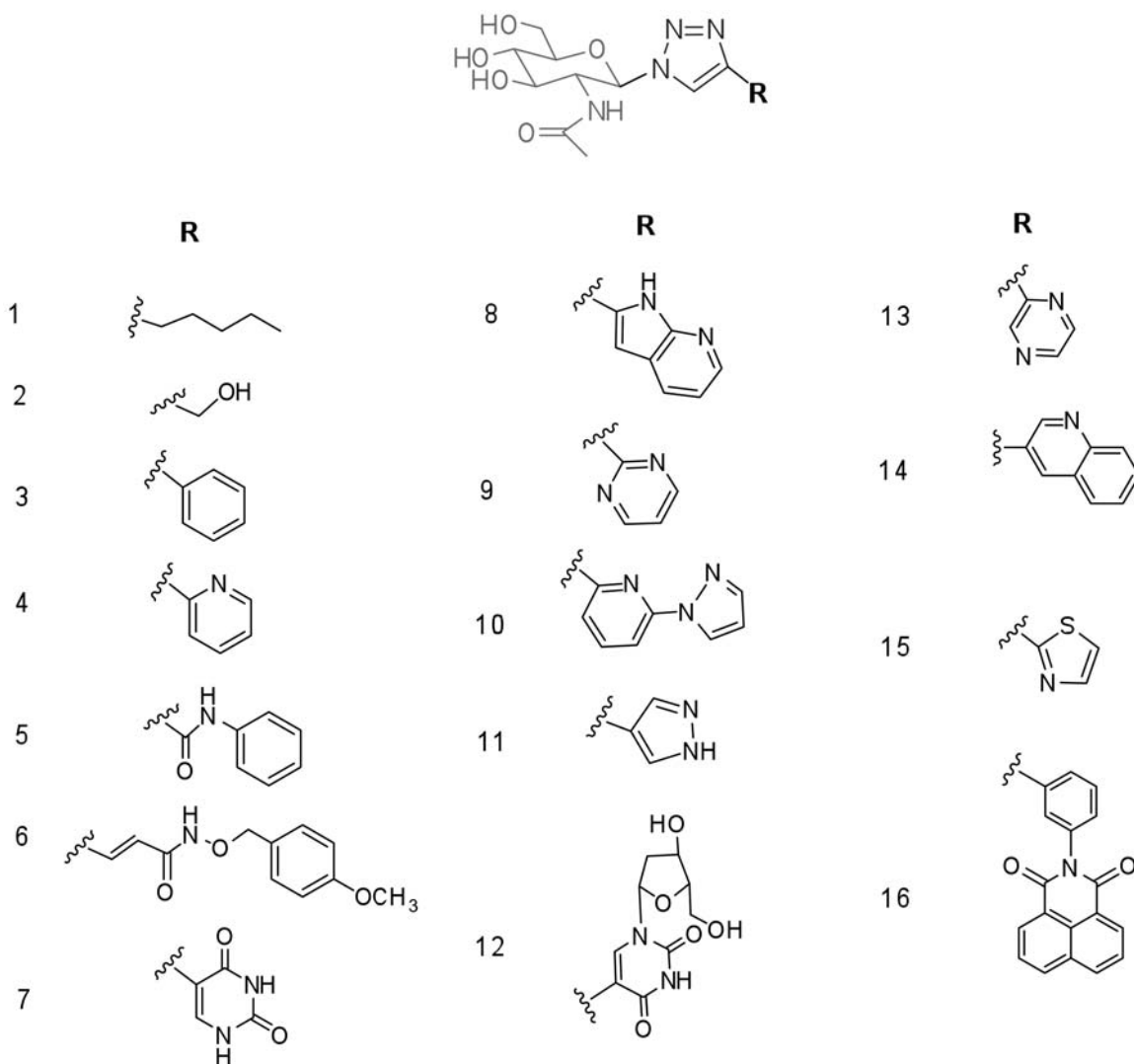


Fig. 1. Triazole-linked carbohydrates (1-16).

**Caspase-3 cleavage assay.** Assays were carried out according to the method of Butkinaree [7]. A 5- $\mu$ g sample of fOGA was incubated with 200 U recombinant caspase-3 in caspase-3 reaction buffer (50 mM Hepes, 10 mM DTT, 1% sucrose, 0.1% CHAPS, pH 7.4) for 2.5 h at 37°C. The reaction was stopped by adding an equal volume of 2 $\times$  Laemmli buffer. Cleavage products were separated on 8% SDS-polyacrylamide gel and transferred to a polyvinylidene difluoride membrane (PVDF) (Millipore) for immunoblotting with anti-nOGA antibody.

**Characterization of enzyme activity.** Assays were performed as previously described [15], and 4-MU-GlcNAc was used as substrate. The reaction system (50  $\mu$ l, pH 6.5) contained 50 mM  $\text{NaH}_2\text{PO}_4$ , 100 mM NaCl, 0.1% BSA, 4-MU-GlcNAc (concentrations used: 0.15625, 0.3125, 0.625, 1.25, 2.5, 5.0 mM), compound 4 (concentrations used: 0, 25, 50, 100, 150  $\mu$ M), and 1  $\mu$ l purified recombinant OGA. Assays were initiated by the addition of

enzymes, and the reactions were quenched by the addition of 150  $\mu$ l of quenching buffer (200 mM glycine, pH 10.75) after incubated for 10 min at 37°C. Using a Varian CARY Eclipse fluorimeter 96-well plate system, fluorescence was measured with excitation at 368 nm and emission at 450 nm. The produced 4-MU (4-methylumbelliferone) was determined and compared with a standard curve (obtained with purchased 4-MU). All assays were performed in triplicate under identical conditions.

**Compounds library.** Through Cu(I)-catalyzed “Click” cycloaddition reactions between glycosyl azides and alkynes, a small triazole-linked carbohydrate library (compounds 1-16) was synthesized in our previous work (Fig. 1) [12].

**Model of hOGA.** A model of the catalytic domain of hOGA (residues 63-342) was generated using Geno 3D [9]. Computational docking of PUGNAc against the hOGA model was generated with Autodock 4.2.

## RESULTS AND DISCUSSION

**nOGA, a caspase-3 cleaved OGA isoform, retains glycosidase activity.** A previous report showed that fOGA was cleaved by caspase-3 at D413 during Fas-mediated apoptosis *in vivo* and produced two fragments [7]. In this study, we constructed the plasmid (pET28a-nOGA) for expression of the N-terminal fragment nOGA. To obtain high soluble expression, the concentration of the inducer IPTG (0.01–0.1 mM), induction time (5–15 h), induction temperature (13–25°C), and expression vectors (pET 28a, pET 32a, pGEX 6p-1) were optimized. Unfortunately, no soluble purified nOGA was obtained. After multiple attempts, conditions were modified by growing the cells in LBNB medium, in which 0.5 M NaCl was used for increasing the extracellular osmotic pressure and thus improving the level of expression of recombinant proteins in soluble native form [16]. *Escherichia coli* BL21(DE3) transformed with pET28a-fOGA or pET28a-nOGA was grown in LBNB medium supplemented with 50 µg/ml kanamycin at 37°C overnight. The next day, the inoculated culture was amplified in 1 liter of LBNB medium and induced with 0.025 and 0.1 mM IPTG when grown to the  $OD_{600} \sim 0.6$ . The bacteria were further grown for 20 h at 16°C at 150 rpm and harvested by centrifugation, sonication, and purification. Finally, we obtained the optimized

expression conditions. Briefly, *E. coli* BL21(DE3) cells transformed with pET28a-nOGA were grown in LB broth supplemented with 50 µg/ml kanamycin at 37°C at 200 rpm. Protein expression was induced by the addition of IPTG to a final concentration of 0.025 mM when the  $OD_{600}$  of cultures reached around 0.6. The cultures were further grown for 10 h at 16°C in a shaker at 110 rpm. The cells were harvested by centrifugation and disrupted by sonication. The supernatant of crude extracts was then purified by  $Ni^{2+}$ -NTA chromatography and analyzed by 10% SDS-PAGE. Recombinant nOGA migrated at 58 kDa (Fig. 2a) and was consistent with one fragment produced after caspase-3 cleavage [7]. The other fragment (about 70 kDa) after cleavage might be the C-terminal product of fOGA (Fig. 2b). Western blot analysis further identified this fragment with anti-nOGA antibody (Fig. 2c). After purification, 20–30 mg of soluble, active nOGA with more than 90% purity was obtained from per liter culture.

After purification, we determined the glycosidase activity of nOGA using varied 4-MU-GlcNAc concentrations. Interestingly, nOGA exhibited a  $K_m$  of 0.89 mM and a high *O*-GlcNAcase activity of 0.106 µmol/min per mg (Fig. 3). However, in a previous report Butkinaree [7] considered that nOGA was not an active fragment for *O*-GlcNAcase. We speculated that perhaps the N-terminal

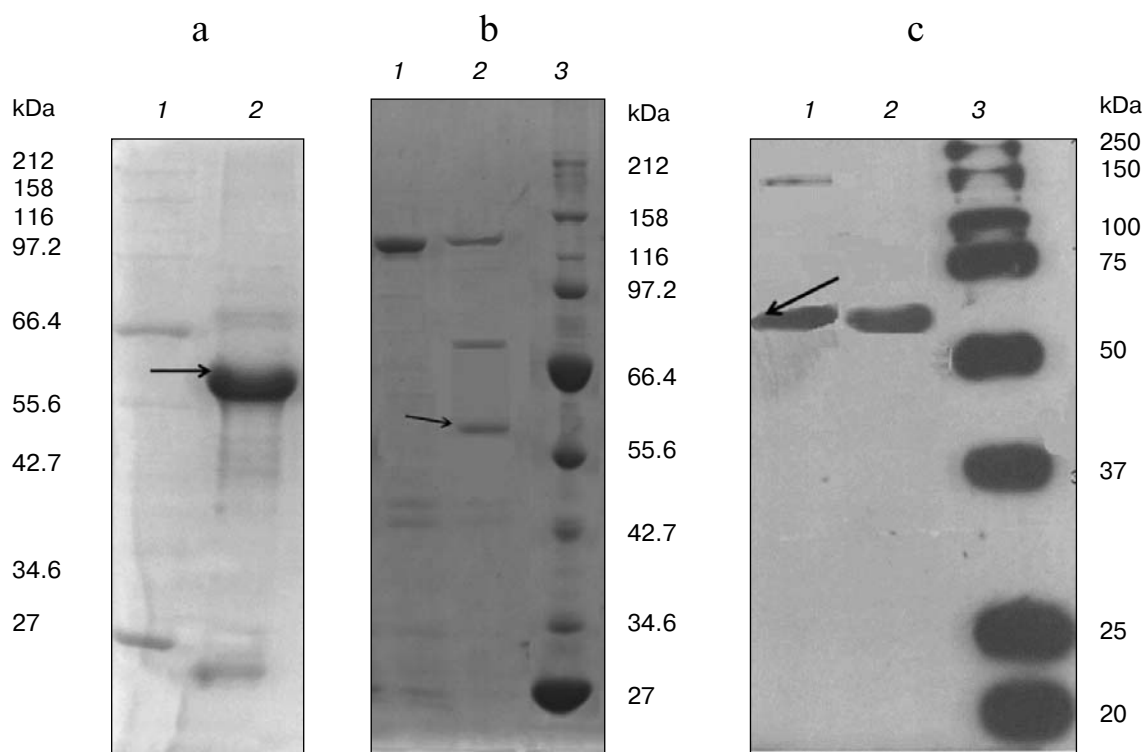


**Fig. 2.** nOGA is the N-terminal product of caspase-3 cleavage. a) Purification of recombinant nOGA from *E. coli*. Lanes: 1) protein marker; 2) nOGA. b) fOGA is cleaved into two fragments by caspase-3. Lanes: 1) recombinant fOGA; 2) recombinant fOGA + caspase-3; 3) protein marker. c) Western blot with anti-nOGA antibody. Lanes: 1) recombinant fOGA + caspase-3; 2) recombinant nOGA; 3) protein marker.

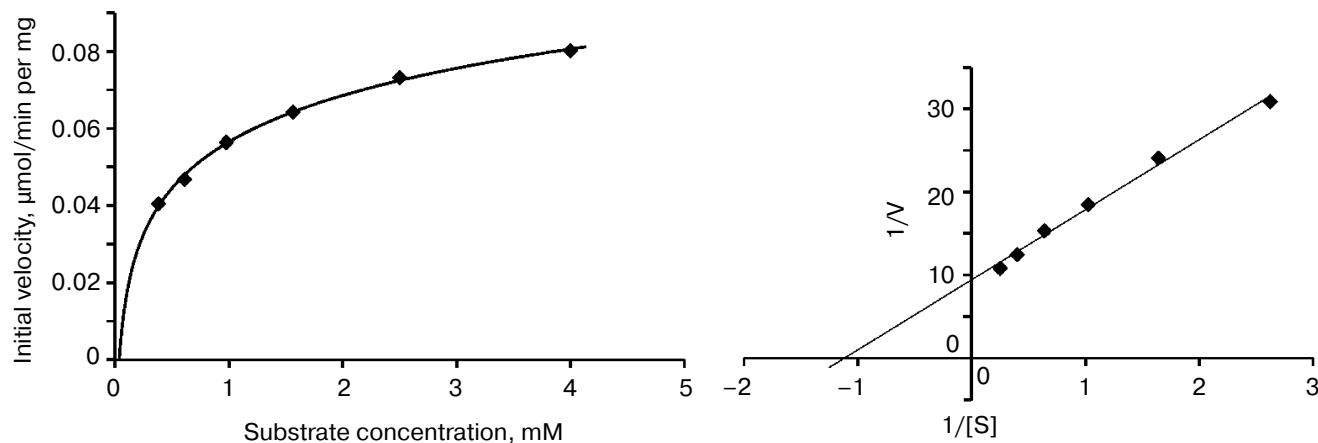


Fig. 3. Activity curve and Lineweaver–Burk plot were generated by varying concentrations of substrate (4-MU-GlcNAc).

fused thioredoxin tag or a less sensitive substrate (*p*NP- $\beta$ -GlcNAc) led to that result.

**Compound 4 showed potent and selective inhibition for nOGA.** A percent inhibition assay was performed as a preliminary screening. In this assay, the inhibition of nOGA activity was compared in the absence and presence of the triazole-linked carbohydrates (**1–16**), which were synthesized in our previous work (Fig. 1) [12], and the results are presented in the table. In comparison, compound **1**, **2**, **6**, and **7** displayed very weak inhibitory potency, compounds **3** and **8–16** showed general inhibition activity, and compound **4** showed the strongest inhibitory potency among the tested compounds.

Subsequently, the inhibition constant ( $K_i$ ) of compound **4** for nOGA was determined in the presence of various concentrations of compound **4** (Fig. 4). It was clear that compound **4** acts as a potent and competitive inhibitor of nOGA with a  $K_i$  of 48  $\mu$ M. In addition, inhibition assays of compound **4** against fOGA and Hex A&B (human lysosomal  $\beta$ -hexosaminidase A&B) were per-

formed. Compound **4** displayed 15-fold lower inhibition for fOGA ( $K_i = 725 \mu$ M) and 10-fold lower for Hex A&B ( $K_i = 502 \mu$ M). Therefore, compound **4** is a potent and selective inhibitor for nOGA.

A number of hydrolytic mechanism studies of OGA and crystallographic studies of homologous bacterial enzymes have demonstrated that the *O*-GlcNAcase active site located in the N-terminal domain, and the catalytic hydrolysis requires aspartic acid residues. Based on the molecular docking of hOGA (63–342) model and PUGNAc (Fig. 5), we found that D174 and D175 were the key catalytic residues. The N-acetylglucosamine of PUGNAc (the same fragment was in the triazole-linked carbohydrate library) contacts with D285, D280, and Y69 by hydrogen bonding, which indicates that the carbohydrates library can be screened for a hOGA candidate inhibitor. The triazole structure may be correlated with the inhibition effect. Briefly, triazole **1** (bearing completely hydrophobic pentyl) and triazole **2** (bearing hydrophilic hydroxymethyl) were unimpor-

Inhibition of nOGA activity by 1H-1,2,3-triazole derivatives at 1 mM concentration

Compound	Inhibition*, %	Compound	Inhibition*, %
1	12.9	9	38.6
2	18.0	10	38.9
3	29.8	11	39.1
4	92.4	12	38.5
5	36.0	13	29.4
6	19.0	14	30.6
7	26.5	15	32.8
8	40.4	16	38.9

\* Values are averages of at least three experiments, and errors are in the range of  $\pm 0.2$ –3% of the reported value.

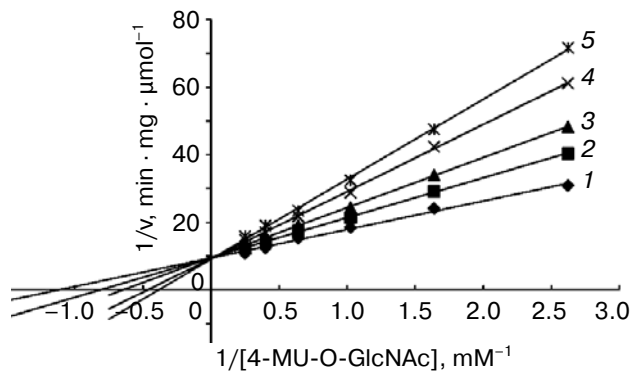


Fig. 4. Lineweaver–Burk analysis of nOGA with compound **4** at concentrations of 0, 5, 10, 50, and 100  $\mu$ M (lines 1–5, respectively).

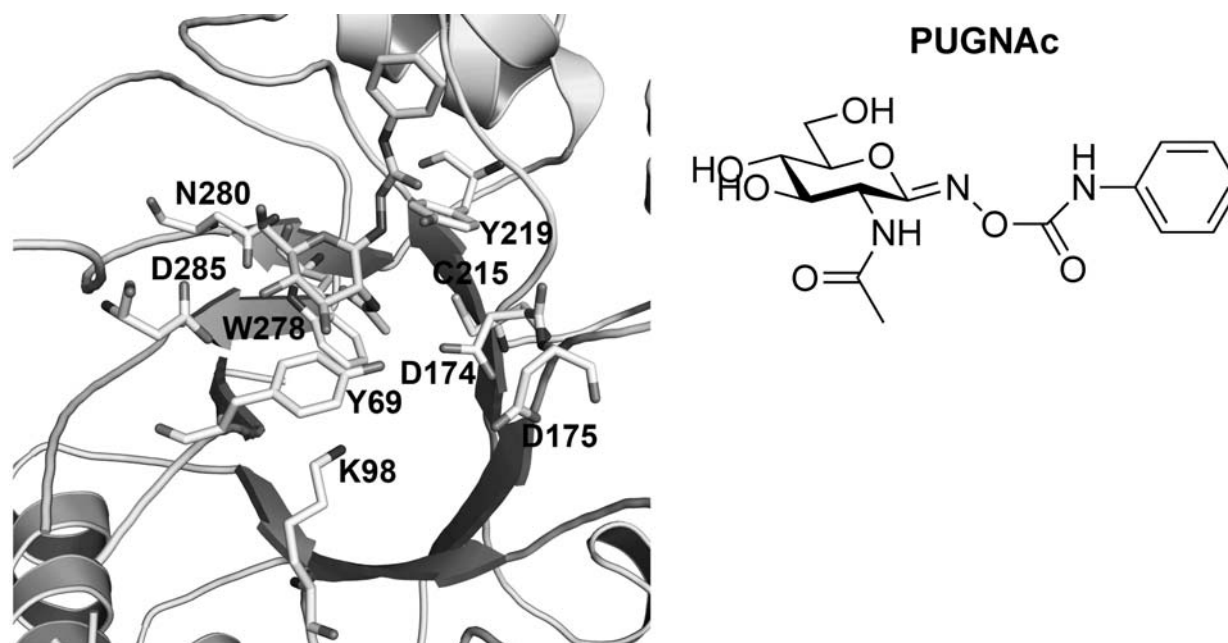


Fig. 5. Active site prediction of human sOGA modeling with its inhibitor PUGNAc.

tant for the interaction with the enzyme molecule. Triazole **3** with phenyl was important due to the ability of phenyl participating in  $\pi$ - $\pi$  stacking with the solvent-exposed Y219. It is noteworthy that triazole **4** can form an important H-bond with carboxylates and other H-bond donors in the appropriate site owing to the lone electron pair on the N atom of pyridyl, and interact with the solvent-exposed Y219 by  $\pi$ - $\pi$  stacking. Although triazoles **8-16** bearing heterocyclic groups and compounds **5** and **6** with aromatic ring can participating in  $\pi$ - $\pi$  stacking with the solvent-exposed Y219, unfavorable H-bond forming has an effect on the enzyme activity in a certain region.

In summary, biological screening of the triazole-linked carbohydrates (**1-16**) revealed that compound **4** is a potent and selective inhibitor for nOGA ( $K_i = 48 \mu\text{M}$ ) over fOGA ( $K_i = 725 \mu\text{M}$ ) and Hex A&B ( $K_i = 502 \mu\text{M}$ ). Based on the study of structure-activity relationships of these triazoles bearing various substituents, we suppose that important hydrogen bonds formed in the appropriate site and  $\pi$ - $\pi$  stacking with the solvent-exposed tyrosine are necessary for a potent inhibitor of nOGA. Meaningfully, compound **4** can be used as a valuable tool to investigate the role of nOGA in cellular apoptosis and the features of different OGA isoforms.

We thank Dr. G. W. Hart from the Medical School of Johns Hopkins University for kindly providing the human O-GlcNAcase cDNA.

This work was supported by the National Basic Research Program of China (973 Program: No.

2007CB914403), Natural Science Foundation of China (No. 31000371, 91013013), and the Fundamental Research Funds for the Central University (65011091).

## REFERENCES

1. Torres, C. R., and Hart, G. W. (1984) *J. Biol. Chem.*, **259**, 3308-3317.
2. Hart, G. W., Housley, M. P., and Slawson, C. (2007) *Nature*, **446**, 1017-1022.
3. Wells, H., Vosseller, K., and Hart, G. W. (2001) *Science*, **291**, 2376-2378.
4. Macauley, M. S., and Vocadlo, D. J. (2010) *Biochim. Biophys. Acta*, **1800**, 107-121.
5. Comtesse, N., Maldener, E., and Meese, E. (2001) *Biochem. Biophys. Res. Commun.*, **283**, 634-640.
6. Toleman, C., Paterson, A. J., Whisenhunt, T. R., and Kudlow, J. E. (2004) *J. Biol. Chem.*, **279**, 53665-53673.
7. Butkinaree, C., Cheung, W. D., Park, S. J., Park, K., Barber, M., and Hart, G. W. (2008) *J. Biol. Chem.*, **283**, 23557-23566.
8. Macauley, M. S., and Vocadlo, D. J. (2009) *Carbohydr. Res.*, **344**, 1079-1084.
9. Li, J., Huang, C. L., Zhang, L. W., Lin, L., Li, Z. H., and Wang, P. (2010) *Biochemistry (Moscow)*, **75**, 938-943.
10. Srinivasan, R., Uttamchandani, M., and Yao, S. Q. (2006) *Org. Lett.*, **8**, 713.
11. Rossi, L. L., and Basu, A. (2005) *Bioorg. Med. Chem. Lett.*, **15**, 3596-3599.
12. Li, T., Guo, L., Zhang, Y., Wang, J., Li, Z., Lin, L., Zhang, Z., Li, L., Lin, J., Zhao, W., Li, J., and Wang, P. G. (2011) *Carbohydr. Res.*, **346**, 1083-1092.
13. Bradford, M. M. (1976) *Anal. Biochem.*, **72**, 248-254.

14. Laemmli, U. K. (1970) *Nature*, **227**, 680-685.
15. Macauley, M. S., Whitworth, G. E., Debowski, A. W., Chin, D., and Vocadlo, D. J. (2005) *J. Biol. Chem.*, **280**, 25313-25322.
16. Oganessian, N., Ankoudinova, I., Kim, S. H., and Kim, R. (2007) *Protein Expr. Purif.*, **52**, 280-285.
17. Rao, F. V., Dorfmueller, H. C., Villa, F., Allwood, M., Eggleston, L. M., and Aalten, D. M. (2006) *EMBO J.*, **25**, 1569-1578.
18. Toleman, C., Paterson, A. J., and Kudlow, J. E. (2006) *Biochim. Biophys. Acta*, **1760**, 829-839.
19. Whitworth, G. E., Macauley, M. S., Stubbs, K. A., Dennis, R. J., Taylor, E. J., Davies, G. J., Greig, I. R., and Vocadlo, D. J. (2007) *J. Am. Chem. Soc.*, **129**, 635-644.
20. Dorfmueller, H. C., Borodkin, V. S., Schimpl, M., Shepherd, S. M., Shpiro, N. A., and Aalten, D. M. (2006) *J. Am. Chem. Soc.*, **128**, 16484-16485.
21. Shanmugasundaram, B., Debowski, A. W., Dennis, R. J., Davies, G. J., Vocadlo, D. J., and Vasella, A. (2006) *Chem. Commun.*, **8**, 4372-4374.